JOURNAL OF PROPULSION AND POWER
Vol. 19, No. 5, September–October 2003

Some Aspects of Chemical Kinetics in Chapman–Jouguet Detonation: Induction Length Analysis

Tianfeng Lu,* Chung K. Law,† and Yiguang Ju‡
Princeton University, Princeton, New Jersey 08544

The influence of complex chemical kinetics on the induction length in Chapman–Jouguet detonation was studied, with emphases on hydrogen chemistry and applications in pulse detonation engines (PDEs). Problems studied include the role of branching–termination reactions on the overall reaction rate, the reduction of the detailed hydrogen oxidation mechanism to simpler ones without compromising comprehensiveness of description, the coupled influence of chemical reactivity and the upstream speed of sound on ignition, and the use of hydrogen as a potential ignition enhancer. Results show that the presence of the pressure-sensitive and temperature-insensitive three-body termination reactions can significantly prolong the ignition delay, that an operation map for PDE operation can be constructed based on the crossover temperature so that operation regimes with excessively long ignition delays can be avoided, and that while the extent of chemistry reduction for the hydrogen/air PDE system depends on the degree of parametric comprehensiveness required, a two-step reduced mechanism appears to be adequate for near-stoichiometric descriptions. Furthermore, it is demonstrated that the benefit of the fast hydrogen chemistry is moderated by hydrogen's high speed of sound, which reduces the detonation Mach number and thereby the postshock temperature.

Introduction

STUDIES of the Chapman–Jouguet detonation can be conducted at several levels of detail. At the simplest level of adiabatic propagation and downstream chemical equilibrium, the detonation velocity can be readily determined without knowledge of chemical kinetics. The predicted velocity also agrees well with experimental observations for propagation in off-limit situations.[1]

Finite rate kinetics and the associated kinetic mechanisms are needed, however, in the study of two aspects of detonation phenomena. The first is concerned with near-limit propagations leading to quenching of the detonation wave. The quenching agent can be volumetric heat loss, frictional and heat loss at the wall of the detonation tube, or wave curvature. Combustion is nonadiabatic and complete reactant consumption is not achieved at the sonic state. The second aspect concerns determining the induction length for adiabatic propagation and using it to estimate such global detonation parameters as the cell size of steady propagation and the wave curvature at quenching.[2]

The simplest description of chemistry is that of a one-step irreversible reaction. Theories and detailed computations have been conducted on various aspects of detonation based on this assumption, and useful insights have been gained. At the same time, however, it is also recognized that such a simplification inherently cannot quantitatively describe many detonation responses of interest, especially in view of the sensitive Arrhenius nature of the reaction rate to temperature variations. Furthermore, ad hoc correlations of the experimental results with adjustable kinetic parameters such as the overall activation energy and reaction order are applicable only in limited ranges of the system and thermodynamic parameters.

What is more serious in the use of one-step chemistry is that it precludes the influence of chain-branching–termination mechanisms that are invariably multistep in nature. A prominent example is the three explosion limits of the hydrogen/oxygen system, which shows that for a homogeneous mixture at a fixed temperature, increasing the system pressure from a low value of nonexplosion can render it to be explosive, nonexplosive, and explosive again. Another example is the recent observation that ignition can be largely achieved via radical proliferation instead of thermal feedback.[3,4] Such a phenomenon again cannot be described by a one-step overall reaction.

The primary objective of the present study is to demonstrate the intrinsic importance of chemistry, mostly beyond the one-step approximation, through an induction length analysis of the CJ wave. Specifically, we shall study three problems that demonstrate the effects of various aspects of chemistry on the induction length. The first is an investigation of the influence of the nonmonotonic explosion limits of the hydrogen/oxygen system on the induction length. The analysis identifies specific relations between the transition boundaries and the induction length and yields an operation map that indicates the transition boundaries in the initial-temperature T_1, initial-pressure p_1, and fuel equivalence ratio ϕ space, across which drastic changes in the induction length are expected. The second problem explores the extent to which the detailed hydrogen/oxygen mechanism can be reduced and still maintain reasonable predictive capability. The third compares the induction length of hydrogen with those of hydrocarbon fuels, namely ethylene and heptane, and investigates the potential of using small amounts of hydrogen as an ignition enhancer. The competing effects of chemistry and the speed of sound of the gaseous medium are identified.

Model of Numerical Simulation

Calculation of the induction length involves first determining the CJ velocity for the given T_1, p_1, and ϕ. The numerical method adopted to solve the CJ detonation velocity is well established, and STANJAN[5] was used to calculate the CJ detonation velocity in the present study.

Once the detonation velocity is obtained, the postshock temperature T_2, pressure p_2, density ρ_2, and velocity u_2 can be calculated with the normal shock relations in the shock coordinate together with the ideal gas relation:

$$\rho_1 u_1 = \rho_2 u_2 \tag{1}$$

$$p_1 + \rho_1 u_1^2 = p_2 + \rho_2 u_2^2 \tag{2}$$

Received 23 May 2002; revision received 28 May 2002; accepted for publication 9 June 2003.

*Graduate Student, Department of Mechanical and Aerospace Engineering.

†Robert H. Goddard Professor, Department of Mechanical and Aerospace Engineering. Fellow AIAA.

‡Assistant Professor, Department of Mechanical and Aerospace Engineering.

$$h_1 + \tfrac{1}{2}u_1^2 = h_2 + \tfrac{1}{2}u_2^2 \tag{3}$$

$$p = \rho RT \tag{4}$$

where h is the specific enthalpy, and the subscripts 1 and 2 respectively indicate the state ahead of and immediately behind the shock.

Using the solution at state 2 as the initial condition, the structural evolution of the postshock homogeneous mixture undergoing chemical reaction can be traced through numerical integration of Eqs. (5–8), as follows:

Continuity:

$$\frac{\mathrm{d}}{\mathrm{d}x}(\rho u) = 0 \tag{5}$$

Species conservation:

$$\frac{\mathrm{d}}{\mathrm{d}x}(\rho u Y_k) = w_k W_k, \qquad k = 1, 2, \ldots, K \tag{6}$$

Momentum conservation:

$$\frac{\mathrm{d}}{\mathrm{d}x}(p + \rho u^2) = 0 \tag{7}$$

Energy Conservation:

$$\frac{\mathrm{d}}{\mathrm{d}x}\left[\rho u\left(h + \frac{u^2}{2}\right)\right] = 0 \tag{8}$$

where x is the spatial coordinate with the origin at the shock, the subscript k designates the kth species, Y is the mass fraction, K is the total number of species, w is the molar production rate, and W is the molecular weight.

Once the structure of the detonation wave is calculated, the induction length can be obtained as the location of the maximum temperature gradient. For quantitative relevance, we shall adopt the operating parametric ranges of the pulse detonation engine (PDE) and pulse detonation rocket engine in our demonstration. Calculations were therefore performed for an initial temperature range from 298 to 500 K, initial pressure range from 0.1 to 5 atm, and equivalence ratio range from 0.5 to 1.5. The relative error tolerance for the numerical integration was set to be 10^{-6}.

The calculation employed detailed oxidation reaction mechanisms for hydrogen,[6] ethylene,[7–9] and heptane.[10,11] Discussion on their validation and comprehensiveness can be found in the respective references. Air is the oxidizer for all the fuels studied.

Second-Limit Effects

It is well established that there are three explosion limits for hydrogen/air mixture, known as the Z curve on a pressure vs temperature plot.[3] Below the first explosion limit, the pressure is very low, and the chain-branching effect can be suppressed by the loss to surfaces, which is strongly system dependent. The explosive regime above the first explosion limit is controlled by the branching and propagating reactions involving the generation of H, O, and OH radicals. The controlling chain-branching reaction is $\mathrm{H} + \mathrm{O_2} \rightarrow \mathrm{O} + \mathrm{OH}$ (R1). The rate of chain branching, however, is moderated by the chain "termination" reaction $\mathrm{H} + \mathrm{O_2} + \mathrm{M} \rightarrow \mathrm{HO_2} + \mathrm{M}$ (R9) as pressure further increases, because the $\mathrm{HO_2}$ radical produced is relatively stable at low temperature, where M is a third body. With increasing pressure, the collision frequency and, hence, rate of the three-body termination reaction R9 greatly increases relative to that of the two-body branching reaction R1. Consequently, in the second limit, reaction R9 becomes sufficiently competitive, and radical explosion is suppressed because the chain-termination effect balances the chain-branching effect. It can then be shown that the second limit is given by the relation $2k_1 = k_9[M]$, which uniquely relates the system pressure and temperature and yields the crossover temperature. Finally, with further increase in pressure, the concentration of the relatively inactive $\mathrm{HO_2}$ radical becomes high. Their subsequent reactions with either themselves or $\mathrm{H_2}$ will eventually lead to the formation of H and OH radicals and, consequently, explosion beyond the third explosion limit.

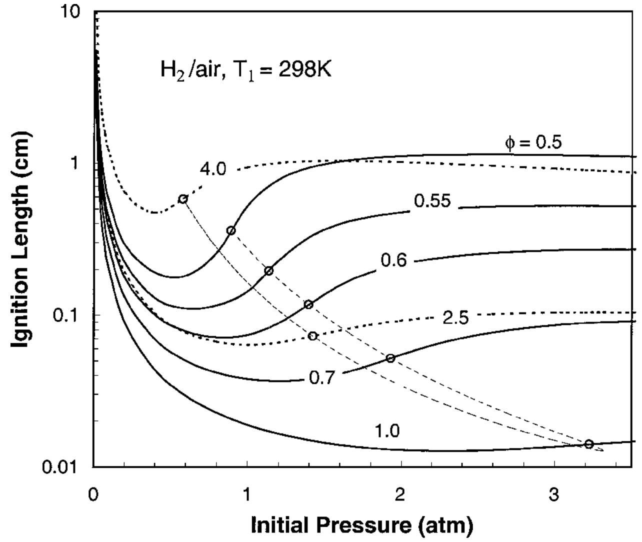

Fig. 1 Dependence of the induction length of hydrogen/air mixtures on initial pressure p_1 and equivalence ratio ϕ; open circles represent the crossover state.

The preceding discussion then implies that the presence of the pressure-sensitive but temperature-insensitive third-order termination reaction could substantially reduce the overall reaction rate as pressure increases. In particular, for a sufficiently weak mixture with a correspondingly low postshock temperature and weakened temperature-sensitive branching reaction R1, the termination reaction R9 is expected to exert a stronger influence. Indeed, it was found[12] that the induction length could actually increase with increasing pressure, and the minimum induction length was found[12] to correspond to the state of the crossover temperature given by Eq. (9). To further examine the aforementioned effect, Fig. 1 shows the calculated induction length for $\mathrm{H_2}$/air mixtures of various equivalence ratios and initial pressures p_1, at a fixed initial temperature T_1 of 298 K. It is seen that the induction length initially decreases and then increases with increasing p_1 and, hence, increasing postshock pressure p_2, in accordance with the result of Ref. 12. However, the present result also shows that, contrary to the suggestion of Ref. 12, the states of the crossover temperature do not correspond to those of the minimum induction length. Rather, they are basically located at the inflection points of these curves, as shown by the symbols in Fig. 1. This result is reasonable because the state of the crossover temperature is that of transition of chemical reactivity from one dominated by chain branching to one dominated by chain termination. A transition of this nature is expected to exhibit an inflection-point behavior in system responses.

Figure 1 further demonstrates the sensitivity of ignition to the ambient pressure for weak, sufficiently off-stoichiometric mixtures in that a small increase in pressure can shift the system from a state of maximum reactivity, indicated by the minimum induction length, to one that is susceptible to the influence of chain-termination reactions, indicated by the inflection point. This sensitivity diminishes as the mixture becomes more stoichiometric.

Due to the significant increase in induction length above the crossover point, it is prudent that operation of the PDE should avoid such a situation in which the postshock temperature (T_2) and pressure (p_2) would fall above the relation for the crossover temperature, as originally noted by Shepherd.[13] Thus, if we solve the crossover temperature relation together with the shock jump relations (1–4), we can determine the operation boundary between slow and fast branchings as a function of the initial equivalence ratio ϕ, in the system parameter (p_1, T_1) space.

Such a generalized, chemistry-affected operation map is shown in Fig. 2. For a given ϕ, operation with initial states close to or above the transition boundaries between the slow and fast branchings should therefore be avoided.

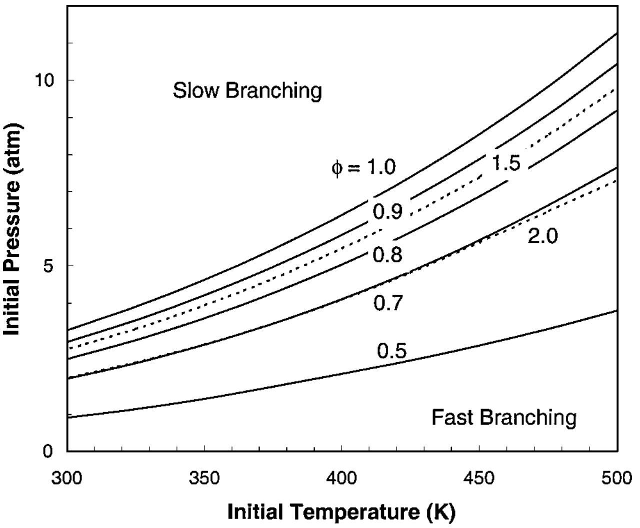

Fig. 2 Hydrogen/air PDE operation map showing boundaries between slow- and fast-branching regimes for given operating parameters T_I, p_I, and ϕ.

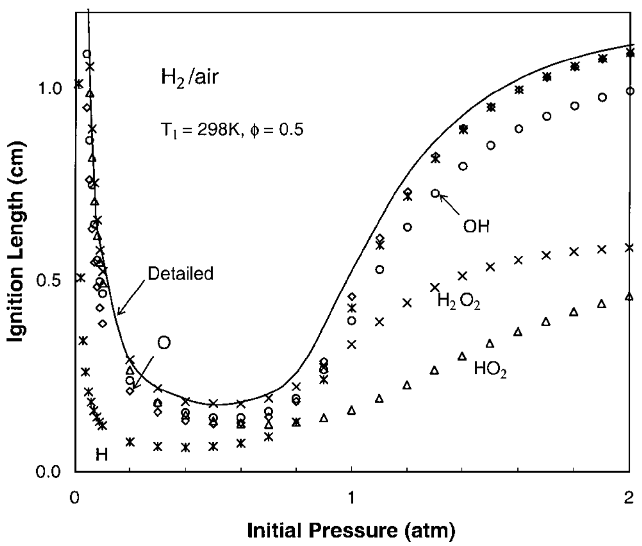

Fig. 3 Comparison of the calculated induction length by using the detailed mechanism vs various five-step mechanisms obtained by assuming one of the five radicals (H, O, OH, HO_2, H_2O_2) is in QSS for ϕ = 0.5.

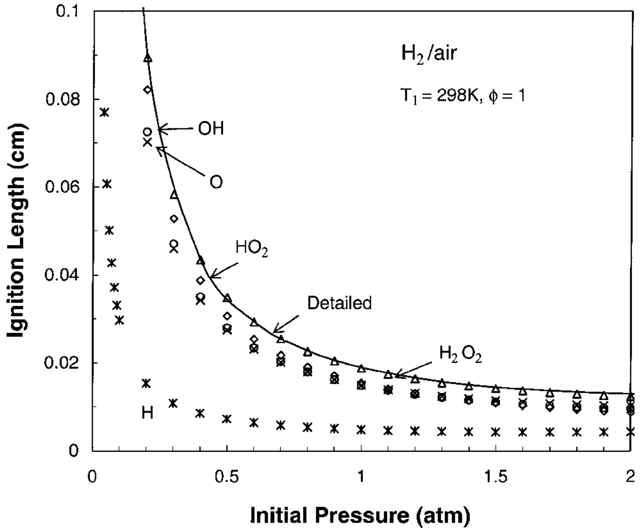

Fig. 4 Comparison of the calculated induction length by using the detailed mechanism vs various five-step mechanisms obtained by assuming one of the five radicals (H, O, OH, HO_2, H_2O_2) is in QSS for ϕ = 1.

Reduced Reaction Mechanisms

In obtaining the aforementioned results, the hydrogen oxidation mechanism used was the detailed one.[6] Although the use of such a detailed mechanism ensures comprehensiveness in the description of all possible outcomes under all possible system operating conditions, the computational requirement can be rather demanding, especially for complex flows such as those involving the cellular detonation wave structure. Thus, there is the incentive to simplify the detailed mechanism through rational approximation without compromising the comprehensiveness of the detailed mechanism.

The particular features of a complex chemical reaction mechanism that lend themselves for approximation are the disparate time scales associated with various groups of reactions. As such, for a given phenomenon or during a particular phase in the progress of the overall reaction, either some individual reactions can be approximated to be in equilibrium, or the concentrations of some species can be approximated to be in quasi-steady state (QSS). These assumptions would reduce the number of species that needs to be solved through differential equations.

A useful algorithm for the systematic reduction of a detailed mechanism using the QSS assumption can be found in Ref. 14. However, due to the very small number of participating species (H_2, O_2, H_2O, H, O, OH, HO_2, H_2O_2) in the hydrogen oxidation mechanism, the reduction can be conducted by simply comparing the performance of different reduced mechanisms, each of which is obtained by assuming only one species to be in QSS. Specifically, because the system consists of eight participating species and two elements, the complete reaction mechanism can be represented by six semiglobal reactions. Thus, by assuming that one of the species is in QSS, the resulting reduced mechanism will consist of five steps. Figures 3 and 4 demonstrate the induction length calculated by using different five-step mechanisms, with equivalence ratios of 0.5 and 1, respectively, under the initial pressure of 1 atm and initial temperature of 298 K. Figure 1 shows that the operating condition for $\phi = 0.5$ and $p = 1$ atm is close to the crossover temperature, whereas that for $\phi = 1$ is well below it. It is seen that, for $\phi = 1$, all radicals except H appear to be in near QSS for all situations. However, for $\phi = 0.5$, HO_2 and H_2O_2 cease to be QSS species for pressures close to or above that of the crossover state such that only the OH and O radicals can be considered to be in QSS. This breakdown of QSS assumption is expected considering the importance of HO_2 and H_2O_2 in establishing the second and third explosion limits. As such, if a reduced mechanism is to be developed for the entire parametric range, only OH and O can be selected as QSS candidates. This selection is different from that in Refs. 15 and 16, in which HO_2 and H_2O_2 were considered to be the best QSS candidates. This does not contradict the present result because the relevant pressures in Refs. 15 and 16 are substantially lower than the present values.

Based on the preceding observations, a four-step reduced mechanism with OH and O as QSS species was generated for application over the entire parametric range including the regime around the second limit, and a two-step reduced mechanism was generated for application in conditions well below the crossover states. The global reactions and the corresponding reaction rates for these two reduced mechanisms are given in the Appendix.

The induction length as a function of p_I has been calculated for the two reduced mechanisms. Figure 5 shows that the four-step mechanism is acceptable throughout the entire initial pressure range for $\phi = 0.5$, whereas the two-step reduced mechanism gives large errors at moderate and high initial pressures, as expected. Figure 6, corresponding to $\phi = 1.0$, shows that the performance of the two-step reduced mechanism is acceptable for all initial pressures.

Hydrogen, Ethylene, and Heptane as Fuels

There are both practical and fundamental motivations in comparing the ignition characteristics of hydrogen, ethylene, and heptane. Practically, hydrogen has been the fuel of choice for high-speed

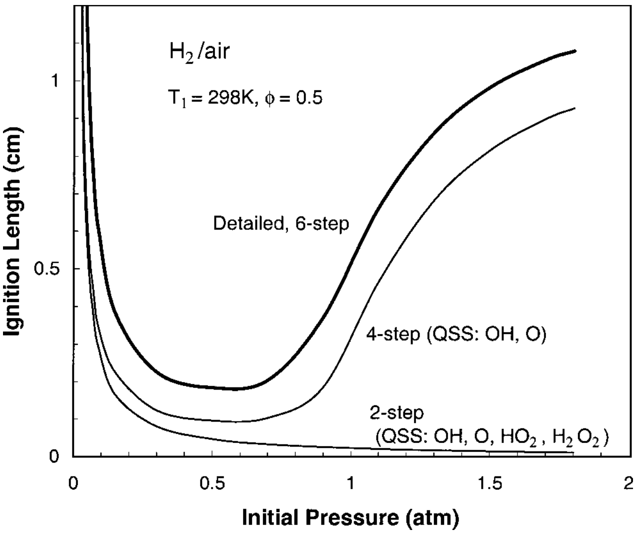

Fig. 5 Comparison of calculated induction length by using detailed mechanism vs two- and four-step reduced mechanisms for $\phi = 0.5$.

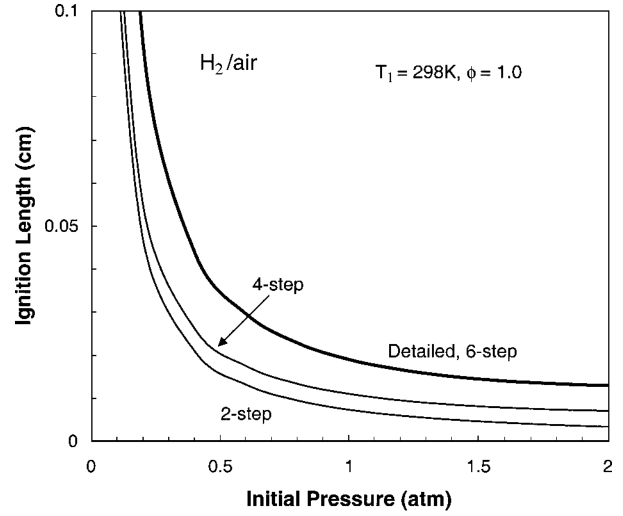

Fig. 6 Comparison of calculated induction length by using detailed mechanism vs two- and four-step reduced mechanisms for $\phi = 1$.

propulsion, whereas heptane is a representative liquid hydrocarbon fuel. Ethylene is a crucial reaction intermediate of higher hydrocarbons and has been used as a surrogate fuel in the simulation of their combustion characteristics. Fundamentally, these three fuels have distinctively different chemical and physical properties. Chemically, they have vastly different reactivities, with hydrogen being the most reactive and heptane the least. Physically, they have very different molecular weights and structures, which in particular would affect the speed of sound and, thereby, the detonation Mach number and the postshock temperature and pressure.

Figure 7 compares the induction lengths of CJ detonation waves of the three fuels as a function of ϕ, for fixed $T_1 = 298$ K and $p_1 = 1$ atm, using different reaction mechanisms. It is seen that, apart from the ethylene results obtained by using the reaction mechanism of Ref. 8, ethylene and heptane have comparable induction lengths that are significantly longer than that of hydrogen. Furthermore, all the fuels exhibit minimum values for ϕ slightly on the rich side of stoichiometry. These trends are anticipated on the basis of chemistry and indeed resemble those of the burning velocities of laminar flames. The dramatically shorter induction length of hydrogen than that of ethylene and heptane is due to hydrogen's higher heat content and faster chemistry.

Figures 8, 9, and 10 respectively show variations of the detonation velocity, upstream speed of sound, and detonation Mach number

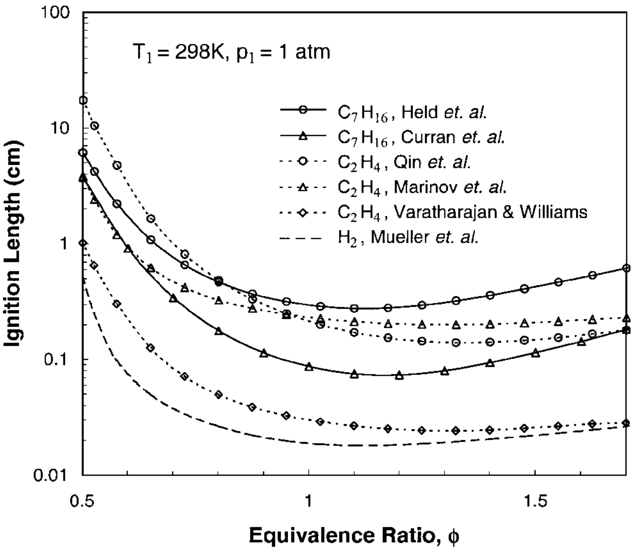

Fig. 7 Dependence of induction length on equivalence ratio for hydrogen, ethylene, and heptane mixtures with air, calculated with different detailed mechanisms.

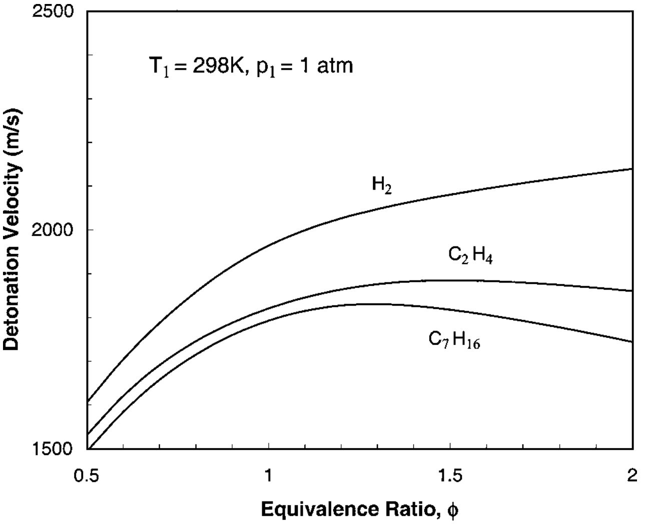

Fig. 8 Dependence of the CJ detonation velocity on equivalence ratio for hydrogen, ethylene, and heptane mixtures with air.

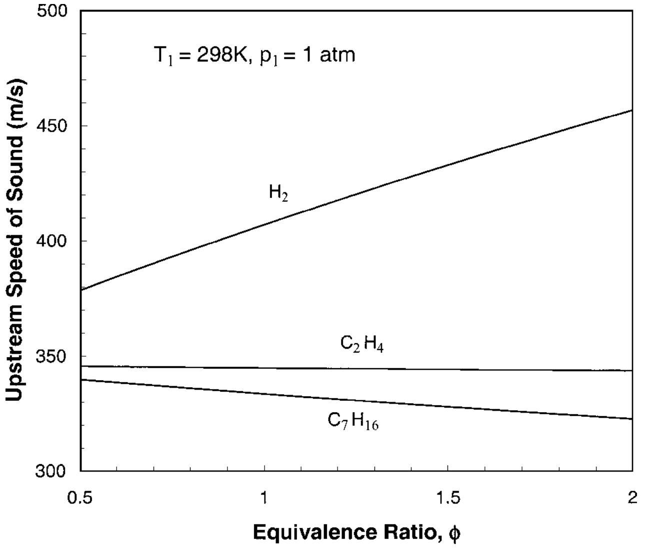

Fig. 9 Dependence of the upstream speed of sound on equivalence ratio for hydrogen, ethylene, and heptane mixtures with air.

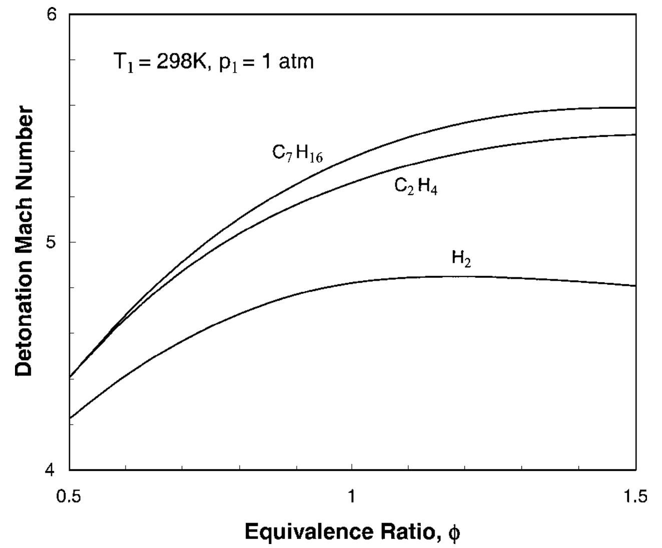

Fig. 10 Dependence of CJ detonation Mach number on equivalence ratio for hydrogen, ethylene, and heptane mixtures with air.

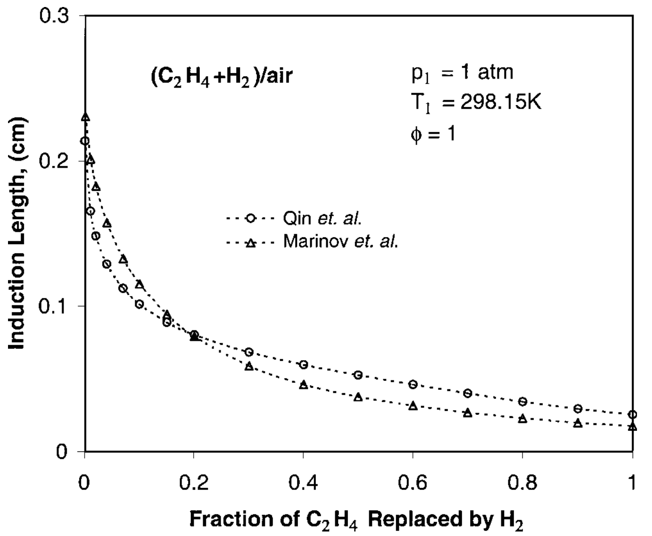

Fig. 11 Induction length for ethylene/air mixtures with varying amounts of added hydrogen.

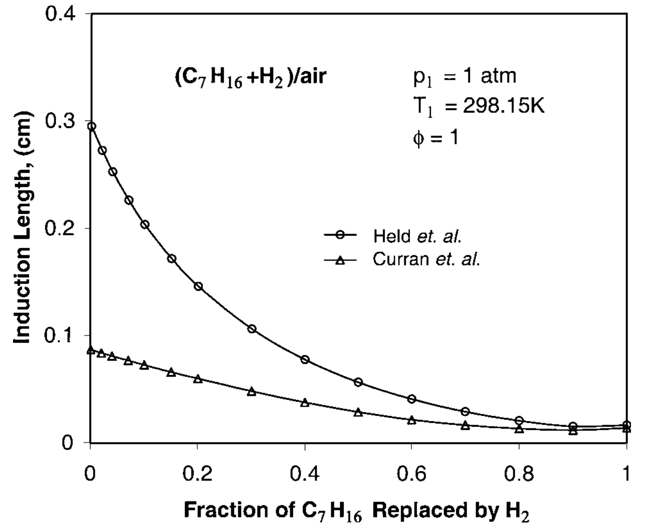

Fig. 12 Induction length for heptane/air mixtures with varying amounts of added hydrogen.

with ϕ for the three fuels. It is seen that the detonation velocity increases in the order of hydrogen, ethylene, and heptane, hence demonstrating the dominating influence of heat content. However, their respective speed of sound not only varies in the opposite manner, but also does not exhibit the same trend with ϕ in that, with increasing ϕ, the speed of sound of hydrogen increases, that of heptane decreases, and that of ethylene is minimally affected. These are primarily effects of molecular weight in that hydrogen is the lightest and heptane the heaviest. Furthermore, because hydrogen and heptane are lighter and heavier than air, respectively, their positive and negative influences on the mixture's speed of sound increase with increasing fuel concentration and, hence, ϕ. The fact that the speed of sound of ethylene is rather insensitive to ϕ is because its molecular weight is close to that of air.

Combining the results of Figs. 8 and 9, Fig. 10 shows that the upstream Mach numbers of the three fuels vary opposite to their respective detonation velocities in that, because of the speed of sound effect, the hydrogen detonation wave has the lowest strength, whereas that of heptane has the highest. Consequently, the hydrogen mixture has a chemically weaker postshock environment to achieve ignition than the ethylene and heptane mixtures. Thus, even though hydrogen is significantly more chemically reactive than heptane and ethylene, its efficiency in initiating reaction in the postshock environment is moderated by its smaller detonation Mach number.

Hydrogen as Additive to Hydrocarbons

Because of the strong reactivity of hydrogen, it has been suggested for use as an additive to reduce the induction length of hydrocarbon fuels. However, in light of the negative effect of the speed of sound on the postshock thermodynamics environment, it is not clear if the benefit of enhanced reactivity can be readily realized for all conditions.

Figure 11 shows the induction lengths of mixtures of ethylene and hydrogen at $T_1 = 298$ K, $p_1 = 1$ atm, and under overall stoichiometric condition, using the ethylene oxidation mechanisms of Refs. 7 and 9. The comparison is conducted by replacing a fraction of ethylene with a stoichiometrically equivalent amount of hydrogen; that is, 1 mol of ethylene is replaced with 6 mol of hydrogen, and as such the overall equivalence ratio remains unchanged. It is seen that whereas the different mechanisms yield noticeable differences in the induction length, the overall trend of adding hydrogen to ethylene is the same. Specifically, while addition of a small amount of hydrogen to ethylene can significantly shorten the induction length, this effect becomes weaker with further addition. These results are reasonable in that, with small amount added, the negative effect of speed of sound is minor such that the chemistry effect dominates, causing the observed large sensitivity in the reduction of the induction length. However, with a larger amount of added hydrogen, the strong kinetic effect is moderated by the reduced Mach number and, hence, the weakened postshock environment, leading to a more gradual reduction in the induction length.

When the hydrocarbon fuel is heptane, the displacement of 1 mol of heptane requires 22 mol of hydrogen to maintain stoichiometry. Due to the large amount of hydrogen used, the speed-of-sound effect becomes prominent even for a small amount of heptane replaced. This substantially moderates the sensitivity of the induction length throughout the range of hydrogen replacement, as shown in Fig. 12, where we used the heptane mechanisms of Refs. 10 and 11 in the calculation. The substantial difference between the calculated results obtained by using different reaction mechanisms, both here and in Fig. 7, demonstrates the importance of chemistry and the unsatisfactory state of knowledge in the reaction mechanisms of such important fuels as ethylene and heptane.

To further demonstrate the competing effects of chemical kinetics and speed of sound, Figs. 13 and 14, respectively, show the induction length and postshock temperature of heptane and hydrogen mixtures for different fixed incident shock velocities, using the mechanism of Ref. 10. It is seen that for a fixed incident shock velocity D, the addition of a small amount of hydrogen indeed reduces the induction length due to the fast chemistry under high

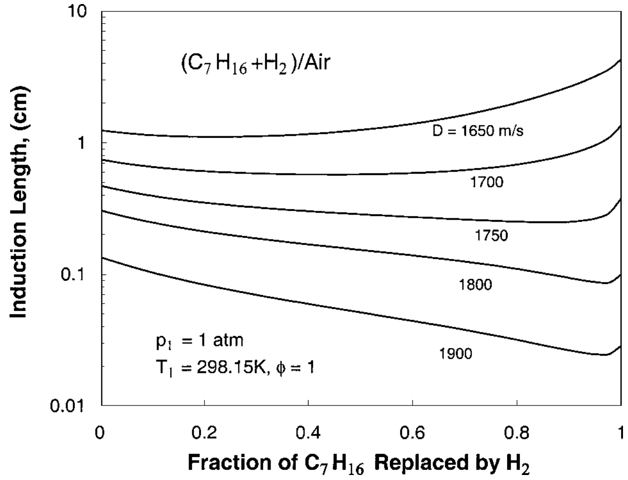

Fig. 13 Induction length for heptane/air mixtures with varying amounts of added hydrogen for fixed incident shock velocities.

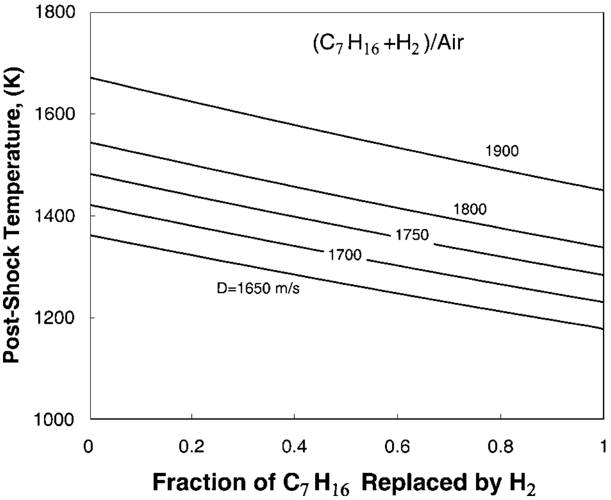

Fig. 14 Postshock temperature for heptane/air mixtures with varying amounts of added hydrogen for fixed incident shock velocities.

postshock temperatures. Furthermore, with increasing hydrogen addition, there exists a minimum induction length beyond which the speed-of-sound effect becomes important, causing it to increase. It is also seen that, as the incident shock velocity increases, the state of the minimum induction length shifts toward the hydrogen side. This is reasonable because increasing incident shock velocity results in higher postshock temperature, which enhances the chemistry effect and thereby delays the onset of the influence of the speed-of-sound effect.

Conclusions

In the present study we investigated several chemistry-related issues pertaining to the structure and propagation of detonation waves, with emphasis on hydrogen oxidation. Whereas the vehicle of study is the induction length of the CJ wave, and the numerical calculations were conducted for system parameters of interest to PDE applications, the concepts and order-of-magnitude effects identified are expected to be of general utility.

Specifically, confirming previous studies, we again demonstrated for hydrogen oxidation the important role of branching–termination chain mechanisms in the overall reaction rate and showed that increasing pressure can significantly moderate its progress. The concept of crossover temperature, which was shown to have an inflexion point influence on the induction length to pressure variations, was applied to derive an operation boundary in terms of p_1, T_1, and ϕ. This boundary provides guidance in avoiding operation regimes for which the induction length could become excessively long.

The potential reduction of the detailed hydrogen/oxygen reaction mechanism to simpler schemes suitable for integration into large-scale computations was also investigated. Results demonstrate that, whereas a four-step reduced mechanism is needed for a comprehensive coverage of the potential range of PDE operations, a two-step mechanism is adequate for near-stoichiometric situations.

By comparing the induction lengths of hydrogen with those of ethylene and heptane, which are representative hydrocarbon fuels, the speed-of-sound effect on the intensity of postshock reactivity is identified, showing that the high reactivity of hydrogen is moderated by the reduced Mach number and, hence, postshock temperature. Consequently, it is suggested that the benefit of using hydrogen as an ignition enhancer is most effective for small amounts of addition so that the speed-of-sound effect is still not significant.

Appendix: Reduced Mechanisms

Four-step Reduced Mechanism

QSS species are OH and O. Non-QSS species are H_2, O_2, H_2O, H, HO_2, and H_2O_2.

Global reactions are as follows:

$$\mathrm{I} : H_2 + O_2 = H + HO_2$$

$$\mathrm{II} : H_2 + HO_2 = H + H_2O_2$$

$$\mathrm{III} : O_2 + H = HO_2$$

$$\mathrm{IV} : 2H_2O_2 = O_2 + 2H_2O$$

Global reaction rates are as follows:

$$w_{\mathrm{I}} = w_2 + w_4 + w_5 - w_8 - w_{10} - w_{13} - w_{14} + w_{15} + w_{18}$$

$$w_{\mathrm{II}} = w_3 - w_4 + w_8 + w_{13} + w_{14} - w_{15} - w_{17} - w_{18}$$

$$w_{\mathrm{III}} = -w_2 + w_3 - 2w_4 - w_5 + 2w_8 + w_9 - w_{11} - w_{12} + w_{13} - 2w_{15} - w_{18} + w_{19}$$

$$w_{\mathrm{IV}} = (w_3 - w_4 + w_8 + w_{13} + w_{16} + w_{19})/2$$

Two-Step Reduced Mechanism

QSS species are OH, O, H_2O_2, and HO_2. Non-QSS species are H_2, O_2, H_2O, and H.

Global reactions are as follows:

$$\mathrm{I} : H_2 = 2H$$

$$\mathrm{II} : 2H_2 + O_2 = 2H_2O$$

Global reaction rates are as follows:

$$w_{\mathrm{I}} = w_2 + w_4 + w_5 - w_8 - w_9 + w_{11} + w_{12} + 2w_{14} - w_{16} - 2w_{17} - w_{18} - 2w_{19}$$

$$w_{\mathrm{II}} = (w_3 - w_4 + w_8 + w_{13} + w_{16} + w_{19})/2$$

Acknowledgments

The work reported herein was supported by the Office of Naval Research and the Air Force Office of Scientific Research.

References

[1] Strehlow, R., *Combustion Fundamentals*, McGraw–Hill, New York, 1984.

[2] Lee, J. H. S., "Dynamic Parameters of Gaseous Detonations," *Annual Review of Fluid Mechanics*, Vol. 16, 1984, pp. 311–336.

[3] Kreutz, T. G., and Law, C. K., "Ignition in Nonpremixed Counterflowing Hydrogen Versus Heated Air: Computational Study with Detailed Chemistry," *Combustion and Flame*, Vol. 104, Nos. 1–2, 1996, pp. 157–175.

[4] Fotache, C. G., Kreutz, T. G., and Law, C. K., "Ignition of Counterflowing Methane Versus Heated Air Under Reduced and Elevated Pressures," *Combustion and Flame*, Vol. 108, No. 4, 1996, pp. 442–470.

[5] Reynolds, W., "The Element Potential for Chemcial Equilibrium Analysis: Implementation in the Interactive Program STANJAN," TR. A-3391, Stanford Univ., Stanford, CA, 1986.

[6] Mueller, M. A., Kim, T. J., Yetter, R. A., and Dryer, F. L., "Flow Reactor Studies and Kinetic Modeling of the H-2/O-2 Reaction," *International Journal of Chemical Kinetics*, Vol. 31, No. 2, 1999, pp. 113–125.

[7] Qin, Z., Lissianski, V. V., Yang, H., Gardiner, W. C., Davis, S. G., and Wang, H., "Combustion Chemistry of Propane: A Case Study of Detailed Reaction Mechanism Optimization," *Proceedings of the Combustion Institute*, Vol. 28, 2000, pp. 1663–1669.

[8] Varatharajan, B., and Williams, F. A., "Ethylene Ignition and Detonation Chemistry, Part I: Detailed Modeling and Experimental Comparison," *Journal of Propulsion and Power*, Vol. 15, No. 2, 2002, pp. 344–351.

[9] Marinov, N. M., Pitz, W. J., Westbrook, C. K., Vincitore, A. M., Castaldi, M. J., and Senkan, S. M., "Aromatic and Polycyclic Aromatic Hydrocarbon Formation in a Laminar Premixed n-Butane Flame," *Combustion and Flame*, Vol. 114, Nos. 1–2, 1998, pp. 192–213.

[10] Held, T. J., Marchese, A. J., and Dryer, F. L., "A Semi-Empirical Reaction Mechanism for n-Heptane Oxidation and Pyrolysis," *Combustion Science and Technology*, Vol. 123, Nos. 1–6, 1997, pp. 107–146.

[11] Curran, H. J., Gaffuri, P., Pitz, W. J., and Westbrook, C. K., "A Comprehensive Modeling Study of n-Heptane Oxidation," *Combustion and Flame*, Vol. 114, Nos. 1–2, 1998, pp. 149–177.

[12] Stamps, D. W., and Tieszen, S. R., "The Influence of Initial Pressure and Temperature on Hydrogen-Air-Diluent Detonations," *Combustion and Flame*, Vol. 83, Nos. 3–4, 1991, pp. 353–364.

[13] Shepherd, J. E., "Chemical Kinetics of Hydrogen-Air-Diluent Detonations," *Prog. Aeronautics and Astronautics*, Vol. 106, Nos. 1–2, 1986, pp. 263–293.

[14] Lu, T. F., Ju, Y., and Law, C. K., "Complex CSP for Chemistry Reduction and Analysis," *Combustion and Flame*, Vol. 126, 2001, pp. 1445–1455.

[15] Balakrishnan, G., Smooke, M. D., and Williams, F. A., "A Numerical Investigation of Extinction and Ignition Limits in Laminar Nonpremixed Counterflowing Hydrogen-Air Streams for Both Elementary and Reduced Chemistry," *Combustion and Flame*, Vol. 102, No. 3, 1995, pp. 329–340.

[16] Ju, Y. and Niioka, T., "Reduced Kinetic Mechanism of Ignition for Nonpremixed Hydrogen/Air in a Supersonic Mixing Layer," *Combustion and Flame*, Vol. 99, Nos. 1–2, 1994, pp. 240–246.